Engr. Fract. Mech., in press (2004)

Simulation of Crack Growth in Ductile Materials

J. A. NAIRN
Material Science and Engineering, University of Utah, Salt Lake City, Utah 84112, USA

Abstract

During crack growth of real materials, the total energy released can be partitioned into elastic and dissipative terms. By analyzing material models with mechanisms for dissipating energy and tracking all energy terms during crack growth, it is proposed that computer simulations of fracture can model crack growth by a total energy balance condition. One approach for developing fracture simulations is illustrated by analysis of elastic-plastic fracture. General equations were derived to predict crack growth and crack stability in terms of global energy release rate and irreversible energy effects. To distinguish plastic fracture from non-linear elastic fracture, it was necessary to imply an extra irreversible energy term. A key component of fracture simulations is to model this extra work. A model used here was to assume that the extra irreversible energy is proportional to the plastic work in a plastic-flow analysis. This idea was used to develop a virtual material based on Dugdale yield zones at the crack tips. A Dugdale virtual material was subjected to computer fracture experiments that showed it has many fracture properties in common with real ductile materials. A Dugdale material can serve as a model material for new simulations with the goal of studying the role of structure in the fracture properties of composites. One sample calculation showed that the toughness of a Dugdale material in an adhesive joint mimics the effect of joint thickness on the toughness of real adhesives. It is expected, however, that better virtual materials will be required before fracture simulations will be a viable approach to studying composite fracture. The approach of this paper is extensible to more advanced plasticity models and therefore to the development of better virtual materials.

Introduction

The toughness, and hence the crack growth properties, of polymers are different when the polymer is in a structure than when the polymer is in bulk form. For example, the toughness of adhesives can depend on the thickness of the adhesive layer (Mostovoy and Ripling, 1966; Mostovoy and Ripling, 1971; Ripling, Motovoy, and Patrick, 1964; Bascom, Cottington, Jones, and Peyser, 1975). In composite materials, both the delamination toughness (Hunston, 1984) and the matrix microcracking toughness (Nairn, 2000) can be dramatically different than the neat matrix toughness. These types of effects are often qualitatively explained in terms of the effect that structure has on yielding processes in polymers, but there are no quantitative models for predicting how constrained yielding affects crack growth. There is a need for such models for guidance in developing polymer-matrix nanocomposites. Because the extent of yielding at a crack tip will have a characteristic length scale, there are likely to be major scaling issues in how yielding is affected by reinforcing the polymer with different length scale fillers. It is likely that scaling issues in the toughness and crack growth properties of nanocomposites will be more dramatic and therefore more important than scaling issues in bulk properties such as stiffness.

One approach to modeling scaling effects on the toughness of polymer composites is by computer methods. It is insufficient, however, to develop traditional crack growth models based on fracture mechanics. Such models input material toughness and model crack growth when the energy release rate (or stress intensity factor) reaches a critical value for the material. This approach requires input of the polymer toughness properties and thus can only model scaling effects if one already knows how toughness is affected by structure. Similarly, cohesive zone models (Barenblatt, 1962; Tvergaard and Hutchinson, 1992; Williams, 2002), which

are popular in crack growth calculations, are no help because one would need to know both the force-displacement law in the crack tip region *and* precisely how that law changes when the polymer is in a structure.

The approach suggested here, is to develop a model or virtual material for which crack growth can be simulated without the need for any input fracture properties. In Griffith's original work on fracture mechanics, a crack was assumed to grow when the energy released by crack growth was equal to the surface energy of the material. This principle was extended to metals and polymers by allowing the critical energy release rate to be a material property that is always much larger than the true surface energy. In polymers, the extra energy is usually assumed to be the result of plastic energy dissipation in the crack tip region. In principle, if one could calculate all plastic energy effects during crack growth, one could simulate crack growth by energy balance between dissipated energy and released energy. This approach is extremely difficult in real materials and no one has succeeded in calculating the toughness of real polymers. If we replace a real polymer by a model material, however, the problem becomes tractable. In a model material, one can choose to *define* all energy dissipation processes. It is then feasible to track all energy effects during crack growth and simulate crack growth without any need for fracture parameters of the material. The crack growth criterion reduces to a condition for energy balance rather than the attainment of some critical crack tip parameter. If a model material can be developed that mimics fracture properties of real materials, the model material could be used in computer simulations to study fracture properties of that material in structures such as composites.

The term "fracture simulation" is used here to mean computer modeling of crack growth in a material where the conditions for crack growth are determined by energy dissipation mechanisms in the material and the requirement for total energy balance. There is no *a priori* specification of an energy required for crack growth, a material toughness, or any crack-tip traction law. Conventional crack growth work with computers is better characterized as doing "fracture calculations" because they numerically solve fracture mechanics models with specified failure criteria. A "fracture simulation" has the potential to model how crack growth properties will change in composites or structures because the energy flow results will depend on the structure. A "fracture calculation" only gives numerical results that depend on the input material toughness and energy flow is determined by that input toughness. The utility of "fracture simulations," however, will depend on the use of a virtual material that reasonably describes energy dissipation processes during crack growth.

The goal of this paper was to demonstrate the process for fracture simulations. The process began by considering basic thermodynamics behind energy balance during stable crack growth of an elastic-plastic polymer under increasing traction loads. It was found that typical methods in plasticity theory lead to crack growth criteria that are indistinguishable from elastic fracture mechanics. The only way to develop virtual plastic materials was to postulate extra irreversible effects that do not appear in traditional plasticity analysis for elastic-plastic fracture methods. Here we derive a differential equation for stable crack growth in terms of global energy release rate and an extra irreversible energy dissipation. The key step to development of a virtual material is to describe a model for the extra irreversible energy. Given such a model, one can undertake fracture simulations. Here the process is illustrated by assuming the extra irreversible energy dissipation is proportional to the plastic energy dissipation from a plastic-flow analysis. This approach can be used with any plasticity theory, but analytical results are possible, and were derived, for a material with a central crack and Dugdale yield zones ahead of each crack tip (Dugdale, 1960; Becker, 1997). The fracture properties of this model material as an infinite sheet were investigated. The effect of finite-sized specimens and of constraint by stiff adherends were investigate by finite element computer simulations. The model material displays some fracture properties characteristic of real polymers. For example, the toughness of the model material used as an adhesive decreases as the joint thickness decreases analogous to experiments in real adhesives (Bascom, Cottington, Jones, and Peyser, 1975). The virtual Dugdale material was used here only for illustration of fracture simulations. It is expected that more realistic virtual materials will be needed before computer simulations will give useful results for scaling effects in the fracture of polymer-matrix composites and nanocomposites.

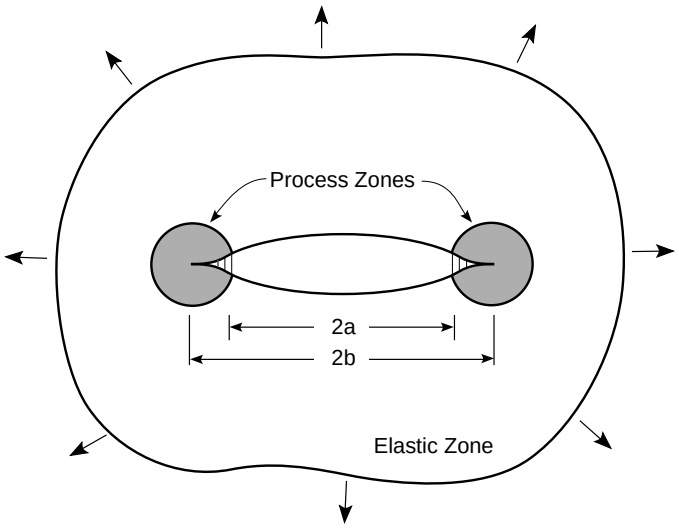

Fig. 1. An arbitrary body subjected to traction loads and containing a single crack of length $2a$ and total damage length of $2b$. The body is divided into an elastic zone and two process zones at each crack tip.

General Analysis

Figure 1 shows a body under load with a crack of length $2a$; the loading and geometry were assumed to be symmetric. Consider crack propagation from crack length $2a$ to $2(a + da)$ that results from some external work done on the sample, w_{ext}. Assuming the crack propagation is sufficiently slow that kinetic energy effects can be ignored and that any dissipated energy leaves the sample as heat, $-q_{ext}$ (isothermal crack growth), the first law of thermodynamics leads to

$$\frac{dw_{ext}}{da} + \frac{dq_{ext}}{da} - \frac{dU}{da} = 4\gamma \tag{1}$$

where U is the total internal energy in the body and γ is the surface energy of the new crack surfaces. All quantities are on a per-unit-thickness basis except for surface properties γ, J and J_p (see below) which are per unit surface area. Equation (1) applies to crack growth during constant or variable tractions or displacements.

Now, partition the body into an elastic zone, where all deformation is purely elastic, and two process zones around the crack tips containing damage zones and all inelastic processes. Each process zone is surrounded by a path through the elastic zone. There is no restriction on the size of the process zones; in fact, the analysis of elastic-plastic fracture is concerned with situations where the zones are large enough such that the body ceases to behave in a globally-elastic manner. Because the elastic zone has no cracks and dissipates no energy, the first law of thermodynamics leads to:

$$\frac{dw_{ext}}{da} - 2\frac{dw_z}{da} - \frac{dU_e}{da} = 0 \tag{2}$$

where w_z is the work done on each process zone by the elastic zone and U_e is the strain energy in the elastic zone. First assume that the process zones are elastic, although they may be non-linear elastic. By definition, J integral is the decrease in potential energy in the zone per unit crack growth (Rice, 1968):

$$J = -\frac{d\Pi_z}{da} = \frac{dw_z}{da} - \frac{dU_z}{da} \tag{3}$$

where Π_z and U_z are the potential energy and strain energy in one process zone. Eliminating w_z in the elastic zone energy balance leads to the obvious result

$$\frac{dw_{ext}}{da} - 2\frac{dU_z}{da} - \frac{dU_e}{da} = 2J \tag{4}$$

which is the standard fracture mechanics result for an elastic material. Because $U = U_e + 2U_z$ and $q_{ext} = 0$ for an elastic material, total energy balance (Eq. (1)) predicts fracture will initiate when

$$J = 2\gamma \tag{5}$$

Under increasing traction loading, J increases with crack length which implies unstable crack growth after initiation (Williams, 1984).

The more interesting problem is when the process zones are elastic/plastic. The usual approach in plastic flow analysis is to partition incremental strain into elastic strain and plastic strain (Hill, 1983). The elastic strain leads to stored strain energy while the plastic strain leads to dissipated energy. In other words, the difference between loading a non-linear elastic process zone and an elastic/plastic process zone is that the elastic energy stored in the non-linear elastic material is partitioned into elastic and plastic energy for the elastic/plastic material, or:

$$\frac{dU_z}{da} = \frac{dU_{z,e}}{da} + \frac{dU_{z,p}}{da} \tag{6}$$

where $U_{z,e}$ and $U_{z,p}$ are the energies stored and dissipated in the process zone. Under isothermal loading, the dissipated energy will eventually be lost as heat:

$$\frac{dq_{ext}}{da} = -2\frac{dU_{z,p}}{da} \tag{7}$$

and the total internal energy is $U = U_e + 2U_{z,e}$. Substituting these results into the total energy balance (Eq. (1)) leads to a fracture criterion for elastic/plastic materials of

$$J_p = 2\gamma \quad \text{where} \quad 2J_p = \frac{dw_{ext}}{da} - 2\frac{dU_{z,p}}{da} - \frac{d(U_e + 2U_{z,e})}{da} \tag{8}$$

This result is identical to the elastic fracture criterion (Eq. (5)) and J_p is energetically equivalent to the elastic J (Eq. (4)); it is written here with subscript p because J refers to an elastic material and may be evaluated by a line integral around a crack tip singularity (Rice, 1968). J_p refers to global energy release rate and is not associated with a crack-tip singularity.

The equivalence of the fracture criteria for initiation of fracture in elastic or elastic/plastic fracture has been noted by others (Atkins, 1999). Prior to crack initiation, there is no distinction, at least in stress-strain properties, between loading a non-linear elastic material and loading an elastic/plastic material. After crack propagation begins, however, a continued equivalence would imply that all plastic energy can be recovered. Because plastic energy is irreversible and not recoverable, the loading paths for non-linear elastic and elastic/plastic fracture must be different. For example, Atkins (1999) has pointed out that extra work must be done during elastic/plastic fracture and that that extra work is related to the energy that would have been recovered had the body been fully reversible elastic. Here an alternative view, albeit physically equivalent to Atkins (1999), is presented based on implied irreversible processes that lead to extra irreversible work.

Similarly, Rice (1976), has noted that continuum approaches based on energy balance seem "to be proposed anew periodically in the elastic-plastic context," but in his view the method can not work due to problems in any exact energy balance. Rice's criticism is based on the loss of a crack-tip singularity resulting in "zero energy surplus from the continuum calculation to be equated to the work of separation." This conclusion is claimed to be identical to the above conclusion that plastic-flow energy balance does not distinguish between elastic and elastic-plastic fracture. Rice further claims that continuum models can not be developed without dealing with the "details of the separation within the fracture process zone." The approach taken here is to develop a continuum model in which those details are described globally by some extra irreversible work. Given a term for extra work, a continuum-based fracture simulation is possible. Consideration of the details of the fracture process zone can then be treated as a separate problem aimed at providing a model for the extra work term.

A physical interpretation of J_p is that it is the work available in the material to propagate a crack. Because elastic deformation is a reversible process, J_p for the elastic material, which is then J, must be the maximum work available. Plastic deformation, however, is irreversible. The energetic equivalence of elastic J and elastic/plastic J_p during crack propagation violates the second law of thermodynamics because the

work available in the irreversible system is the same as the work available in the reversible system. In order to find less work available in the irreversible system, the actual amount of dissipated energy must be larger then the $2dU_{z,p}/dz$ partitioned from plastic-flow analysis. The total dissipated energy can be written as

$$-\frac{dq_{ext}}{da} = 2\left(\frac{dU_{z,p}}{da} + \frac{dU_{z,ex}}{da}\right) \tag{9}$$

where $U_{z,p}$ is the plastic work from a plastic-flow analysis (*i.e.*, energy calculated by Eq. (6)) and $U_{z,ex}$ is some extra dissipated energy (analogous to the extra work in Atkins (1999)). Because $U_{z,p}$ alone leads to a work potential equal to that of the reversible, elastic system, $U_{z,ex}$ can be associated with the total degradation of work potential due to the irreversible nature of plastic deformation. The second law of thermodynamics requires

$$\frac{dU_{z,ex}}{da} \geq 0 \tag{10}$$

Application of total energy balance now leads to a new fracture criterion

$$J_p = 2\gamma + \frac{dU_{z,ex}}{da} \tag{11}$$

where

$$J_p = \frac{dw_z}{da} - \frac{dU_z}{da} - 2\frac{dU_{z,p}}{da} \tag{12}$$

is the maximum work available. Notice that partitioning of dissipated energy as in Eq. (9), allows J_p in Eq. (11) to retain meaning as the maximum work available. The partitioning does not imply that $U_{z,p}$ is reversible; it only implies that traditional plastic-flow methods need to be supplemented with extra irreversible energy to distinguish plastic fracture from elastic fracture. An alternative partitioning, as done by Cherepanov (1968a), is to redefine energy available from elastic terms only,

$$J_e = \frac{dw_z}{da} - \frac{dU_z}{da}, \tag{13}$$

and to move all dissipated terms to the right side of the fracture criterion. The drawback of this approach is that J_e loses an interpretation as maximum work potential because J_e is larger in the irreversible system than in the reversible system. The approach here keeps J_p as a maximum work potential by moving part of irreversible energy to the right side of the equation. As long as all energy is included, the decision of which side of the equation has which terms is arbitrary. The approach here is an attempt to maintain a connection with elastic fracture mechanics methods that use J (see below).

The second law of thermodynamics determines the sign of $dU_{z,ex}/da$, but it is also possible to find the maximum degradation of work. Because crack growth can not create more energy than is released, the extra irreversible energy is limited by

$$0 \leq \frac{dU_{z,ex}}{da} \leq J_p - 2\gamma \tag{14}$$

Substitution of the maximum dissipation into the fracture criterion (Eq. (11)) leads to an identity. In other words, maximum irreversibility implies uncontrolled crack growth. The situation might be viewed crudely as analogous to free expansion of an ideal gas which also occurs under conditions of maximum irreversibility. Although the total irreversible effect is bounded by Eq. (14), the term $dU_{z,ex}/da$ corresponds to the hypothetical work degradation that would occur if the crack were to grow by an amount da. This function is not bounded, but unless there is some load for a given crack length for which Eq. (14) is satisfied, the crack will not grow stably.

A thermodynamic interpretation of the maximum dissipated energy is possible and it has some use. Viewing J_p as the maximum energy available, the maximum extra irreversible energy corresponds to the situation where all the available energy is degraded into heat. Because all dissipation occurs in the process zone, the maximum dissipation occurs when all the work done on the process zones is dissipated into heat (except for the surface energy required by the new crack surface area). Applying the first law of thermodynamics to

the process zones and realizing that maximum irreversibility also implies no internal energy change in that zone, the maximum total dissipated energy is

$$\left(\frac{dq_{ext}}{da}\right)_{max} = 2\left(2\gamma - \frac{dw_z}{da}\right) \tag{15}$$

McCartney (1978) previously considered energy balance during crack growth of an elastic-plastic material and found almost the same results including a need for extra irreversible energy. He considered two models for energy dissipation. His first model assumed dissipated energy was equal to the work done on the process zones which is identical to Eq. (15) except it ignores the surface energy term. Because this dissipated energy exceeds the maximum possible dissipated energy, it led to a fracture growth criterion that was not useful (McCartney, 1978). McCartney's second model is the same as Eq. (6) for the special case of rigid-plastic process zones. His analysis gave the same fracture growth criterion as Eq. (5). Thus, this analysis and McCartney's are essentially identical with McCartney's two models corresponding to the bounds in Eq. (14). The new result here is to provide thermodynamic interpretations of the two dissipation models. Energy dissipation by Eq. (6) corresponds to minimum irreversibility and the fracture properties are indistinguishable from the equivalent reversible material. Energy dissipation by Eq. (15) (which corrects McCartney's first model) corresponds to maximum irreversibility and crack growth occurs spontaneously. A real ductile material is likely to lie between these two extreme models which requires a model for $dU_{z,ex}/da$. McCartney's proposal for $dU_{z,ex}/da$ is discussed below.

The fracture criterion in Eq. (11) is analogous to R curve analysis in fracture (Williams, 1984), but with one important difference. In R curve analysis, the crack grows when $J = R$. The left side of this equation (J) is a function of crack length and load, but the right side (or crack resistance R) is viewed as a material property that is independent of load and only a function of incremental crack length. The crack growth is stable during monotonic loading provided J can continue to equal R. In other words, following non-negative increments in crack length (da) and load ($d\phi$), crack growth is stable provided

$$J(a,\phi) + \left(\frac{\partial J}{\partial a}\right)_\phi da + \left(\frac{\partial J}{\partial \phi}\right)_a d\phi = R(a) + \frac{dR}{da}da \tag{16}$$

Because $J(a,\phi) = R(a)$, this equation can be rearranged into a differential equation for finding crack length as a function of load

$$\frac{d\phi}{da} = \frac{\dfrac{dR}{da} - \left(\dfrac{\partial J}{\partial a}\right)_\phi}{\left(\dfrac{\partial J}{\partial \phi}\right)_a} \tag{17}$$

Because $d\phi/da$ must be positive for monotonic loading and because the denominator is positive, this equation implies that stable crack is only possible if

$$\frac{dR}{da} \geq \left(\frac{\partial J}{\partial a}\right)_\phi \tag{18}$$

This stability criterion is the usual criterion of stable crack growth in elastic fracture (Williams, 1984).

The important difference when analyzing fracture with irreversible energy is that the right side of Eq. (11) is not a material property. The extra irreversible energy dissipation will depend not just on material properties but also on applied load because more energy will be dissipated as applied loads approach yield stress of the material. Defining the right side of Eq. (11) as R^*, to distinguish it from traditional R curves, crack growth and stability conditions can be derived by considered crack growth when $J_p = R^*$. Following Cherepanov (1968a), both J_p and the extra irreversible energy dissipation can be taken as functions of the controlling variables of crack length, a, and applied load, ϕ. Crack growth with energy balance is then defined by

$$J_p(a,\phi) = 2\gamma + \left(\frac{\partial U_{z,ex}}{\partial a}\right)_\phi + \left(\frac{\partial U_{z,ex}}{\partial \phi}\right)_a \frac{d\phi}{da} \tag{19}$$

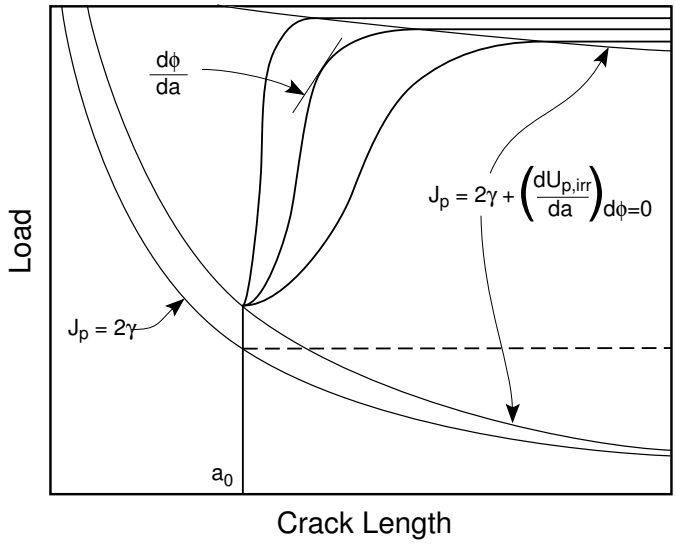

Fig. 2. A schematic view of load as a function of crack length. For real materials there are expected to be two critical curves. Below the lower curve the crack does not grow. The crack initiates at the lower curve and propagates stably until it reaches the upper curve. Above the upper curve crack growth is unstable. For elastic materials, there is only one curve. The crack initiates at that curve and then grows unstably (dashed line).

Rearranging leads to a differential equation for calculating crack length as a function of load during stable crack growth.

$$\frac{d\phi}{da} = \frac{J_p(a,\phi) - 2\gamma - \left(\dfrac{\partial U_{z,ex}}{\partial a}\right)_\phi}{\left(\dfrac{\partial U_{z,ex}}{\partial \phi}\right)_a} \tag{20}$$

Because $d\phi/da$ must be positive for monotonic loading and because the denominator is positive, this equation implies that stable crack is only possible if

$$J_p(a,\phi) \geq 2\gamma + \left(\frac{\partial U_{z,ex}}{\partial a}\right)_\phi \tag{21}$$

This stability criterion extends stability analysis of elastic fracture to problems with irreversible energy dissipation. It is analogous to the stability condition in Cherepanov (1968a). This stability criterion also applies only to load-control conditions which are the conditions used in all example calculations. An analysis of stable crack growth under displacement control would require a revised treatment.

A graphic view of crack initiation and growth can be derived by plotting load as a function of crack length as done in Fig. 2. Superposed on this plot is a plot of three critical functions. The first is for $J_p = 2\gamma$ which gives the load required for a given crack length to initiate elastic fracture. The other two functions are solutions where the equality in the stability criterion in Eq. (21) holds. As found in examples given below, this function is likely to have two solutions that define the boundaries for stable crack growth. The regions between the two solutions have $d\phi/da \geq 0$ which permit stable crack growth; the regions outside the two solutions do not permit stable crack growth (Cherepanov, 1968a). A fracture simulation would proceed as follows:

1. Initially the load will increase from zero until the conditions for crack growth result in crack initiation. In Fig. 2, the initiation step corresponds to the vertical line from zero load up to the lower curve having $J_p = 2\gamma + (\partial U_{z,ex}/\partial a)_\phi$.

2. After initiation, the crack will propagate with some increment in crack length (da) and load ($d\phi$). If this crack growth leads to an area in the $\phi - a$ plot where $d\phi/da \geq 0$, the crack growth can continue stably.

The load-crack length curve can be determined by solution of the differential equation in Eq. (20); *i.e.*, Eq. (20) gives the slope of the crack growth curves. Figure 2 shows three possible crack growth curves. The actual result will depend on the energy dissipation mechanisms in the material. By analyzing a wide range of material properties, this analysis can accommodate a wide range of material behavior from large-scale yielding or ductile failure to small-scale yielding or quasi-elastic fracture.

3. If the crack propagation reaches an upper critical curve, the subsequent growth will be unstable. This region corresponds to the horizontal extension of the crack growth curves from the intersection with the upper $J_p = 2\gamma + (\partial U_{z,ex}/\partial a)_\phi$ curve to large a.

4. For an elastic material, the crack growth will initiate when the curve reaches the lower $J = 2\gamma$ curve. Because $2\gamma = R$ is a constant (*i.e.*, $dR/da = 0$) and $(\partial J/da)_\phi \geq 0$, Eq. (18) implies crack growth under monotonic loading will be unstable. It will follow the horizontal dashed line in Fig. 2.

Prior Stable Crack Propagation Models

An early attempt at calculation of stable crack growth based on plastic energy dissipation was derived by Cherepanov (1968a) and approached similarly by others (Cherepanov, 1668b; McCartney, 1978; Wnuk, 1971).. Cherepanov analyzed energy balance in the elastic zone from which Eq. (2) was expressed as

$$\frac{dw_{ext}}{da} - \frac{dU_e}{da} = 2\frac{dw_z}{da} = 4\gamma^* \tag{22}$$

Cherepanov applied this equation to a complex-potentials analysis of a Dugdale crack and verified that the first equality is true, which must hold. To model crack propagation, this result was equated to an *effective* surface energy term, γ^*. The Cherepanov crack-growth criterion can be recast using fracture mechanics terms, which clarifies the differences from this paper (*c.f.*, Eq. (11)), as:

$$J_p = 2\gamma^* - \frac{dU_{z,p}}{da} \tag{23}$$

Comparison to Eq. (11) shows that the Cherepanov approach is a special case of the general approach above obtained by setting $\gamma^* = \gamma$ and setting the extra irreversible energy dissipation to

$$\frac{dU_{z,ex}}{da} = -\frac{dU_{z,p}}{da} \tag{24}$$

This implied negative value for $dU_{z,ex}/da$ suggests that the Cherepanov approach violates the second law of thermodynamics and therefore does not correctly account for dissipated energy effects. This difficulty can be resolved by including the missing dissipated energy in γ^*, but a reliance on *effective* properties like γ^* limits the use of this approach in simulation of ductile fracture.

McCartney (1978) derived an alternative theory of stable crack growth. As stated above, when McCartney considered energy dissipation by the mechanism identified here as minimum energy dissipation, he derived a result identical to Eq. (5). McCartney recognized this result as having no use in modeling stable crack growth and thus proposed an alternative energy dissipation mechanism. Although McCartney did not discuss extra irreversible energy, his proposed dissipation model exceeds the minimum dissipated energy and can therefore be cast as a prior result that also added extra irreversible energy. For the specific Dugdale material considered, McCartney's model can be recast in the terms of this paper as a model that defines an extra irreversible energy term of

$$\frac{dU_{z,ex}}{da} = \eta + 2\sigma_Y v(a+\epsilon) - \frac{d}{da}\int_a^{a+\epsilon} 2\sigma_Y v(x)\,dx \tag{25}$$

where σ_Y is the yield stress of the material and $v(x)$ is the crack surface displacement in the process zone. The parameters η and ϵ are material properties that are assumed to be constant throughout crack propagation. η is interpreted as the energy dissipated as heat as a result of localized slip process; ϵ defines a crack tip process zone with irreversible dissipation. Although McCartney's extra irreversible energy term is a viable model for fracture simulations, this paper considers an alternate model based on plastic-flow calculations that is not restricted to Dugdale materials.

Example Model for Irreversible Dissipation

By Eq. (20), the problem of simulating crack growth is reduced to the problem of finding J_p and then proposing a model for extra irreversible energy dissipation. The model proposed here is to assume that the extra irreversible plastic energy dissipation is proportional to the minimum dissipated energy or

$$\frac{dU_{z,ex}}{da} = p\frac{dU_{z,p}}{da} \tag{26}$$

where $p \geq 0$ is a parameter defining the degree of irreversibility. To clarify, this model implies that the total energy dissipated as heat is

$$-\frac{dq_{ext}}{da} = (1+p)\frac{dU_{z,p}}{da} \tag{27}$$

In other words, the actual dissipated energy is a sum of the plastic work from plastic-flow analysis and an *assumed* extra irreversible energy required to model plastic fracture.

Although no claim is made about a physical basis of this model, it permits development of fracture simulations and it has several attractive features. First, any analysis for J_p in an elastic-plastic problem will, by necessity, include a calculation of $dU_{z,p}/da$. Thus many existing elastic-plastic crack growth models can be converted into potential models for fracture simulations. Second, it seems reasonable that the capacity for extra irreversible energy dissipation should be related to the capacity for plastic flow. A crude analogy can be drawn with free or irreversible expansion of an ideal gas. In an ideal gas, the irreversible energy lost by free expansion is exactly equal to the heat absorbed by isothermal, reversible expansion (Gaskell, 1995). Compared to an ideal gas, the parameter p might be interpreted as being between 0 and 1 where 0 is for a process with minimum energy dissipation and 1 is for maximum irreversibility. Third, taking extra energy as proportional to plastic-flow energy is analogous to Atkins claim that extra work is related to energy that would be recovered had the body been reversible (Atkins, 1999). Finally, this approach is not tied to any particular model for plastic deformation. Previous models have been specific for Dugdale materials (Cherepanov, 1968a; McCartney, 1978). Although the results below are similarly derived for a Dugdale material (because it permits some analytical results), the approach could be applied to any numerical analysis of elastic-plastic deformation.

Results and Discussion

The Dugdale model for yielding ahead of a crack tip (Dugdale, 1960; Becker, 1997) was used to develop an example virtual material and to illustrate the process of fracture simulations. A Dugdale crack is shown in Fig. 3. The crack is subjected to symmetric, mode I loading far from the crack. The yield zone of length $b-a$ is confined to a line ahead of the crack of length a with the yield criterion that the material will yield when $\sigma_{yy} \geq \sigma_Y$. The attraction of this model is that all stresses and strains can be found by a linear elastic analysis. The method is to treat the yielding as a constant crack-surface traction over a portion of the crack superposed with far-field stress of σ. The size of the yield zone is determined by the requirement that the stress intensity factor at the yield zone tip ($x = b$) is zero. In other words, the negative stress intensity from the crack surface traction just cancels the positive stress intensity from the far-field stress. Two equivalent solutions using complex potentials can be found in Becker (1997) and Cherepanov (1968a).

Simulations of crack growth in a Dugdale material need J_p and the plastic energy dissipation. J_p for a Dugdale crack can be found by a J-integral contour integral along the boundary of the yield zone. The well-known result is (Williams, 1984)

$$J_p = 2\sigma_Y v(a) \tag{28}$$

where $v(a)$ is the displacement at the crack tip ($x = a$) or $2v(a)$ is the total crack opening displacement. Because all the energy that would be stored in an elastic zone is dissipated in a rigid-plastic Dugdale material, the plastic dissipation can be found from Eq. (3):

$$\frac{dU_{z,p}}{da} = \frac{dw_z}{da} - J_p \tag{29}$$

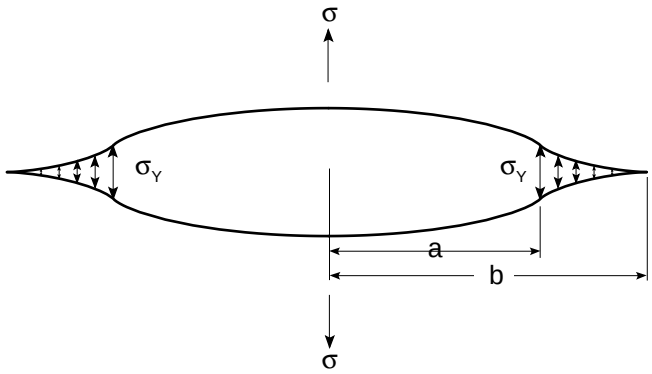

Fig. 3. A crack in a Dugdale material under far-field, mode I loading of σ. The loading causes a line yield zone ahead of the crack tip. The real crack has length a; the yield zone has length $b-a$. The y-direction stress in the yield zone is constant and equal to σ_Y or the yield stress of the material.

where the work term is

$$\frac{dw_z}{da} = \int_a^b 2\sigma_Y \frac{dv(x)}{da} dx \tag{30}$$

It is easy to show that these results simplify to

$$\frac{dU_{z,p}}{da} = \sigma_Y \frac{dA_p}{da} \tag{31}$$

where A_p is the crack area at one crack tip:

$$A_p = \int_a^b 2v(x)\, dx \tag{32}$$

A casual reader might mistake the right side of Eq. (30) as the Dugdale-model J integral which would lead to the incorrect result of $dU_{z,p}/da = 0$. The mistake of this view, beside the physical problem that it implies a plastic material that dissipates no plastic energy (Rice, 1976), is that the displacement derivative in Eq. (30) is with respect to crack length of a propagating crack (da) while the derivative in the J integral is with respect to Cartesian coordinates (dx) for a stationary crack (Rice, 1968). For a propagating crack, which may involve variable tractions, the full derivative of A_p is

$$\frac{dA_p}{da} = \lim_{da\to 0} \frac{1}{da}\left(\int_{a+da}^{b+db} 2v(x,a+da)\, dx - \int_a^b 2v(x,a)\, dx\right) \tag{33}$$

$$= \lim_{da\to 0} \frac{1}{da}\left(-\int_a^{a+da} 2v(x,a)\, dx + \int_{a+da}^{b} 2\big(v(x,a+da)-v(x,a)\big)\, dx + \int_b^{b+db} 2v(x,a+da)\, dx\right) \tag{34}$$

where the second argument on $v(x,a)$ implies displacement as a function of x for a crack of length a. In the limit of small da, the first integral is $-2v(a)$, the last integral is zero, and the equation reduces to

$$\frac{dA_p}{da} = -2v(a) + \int_a^b 2\frac{dv(x)}{da} dx \tag{35}$$

which with Eq. (29) leads to the result in Eq. (31).

The model for stable crack growth thus depends only on the crack opening displacement, $v(x)$, and the length of the yield zone, which are given by (Becker, 1997; Cherepanov, 1968a)

$$v(x) = \frac{(\kappa+1)\sigma_Y a}{8\pi\mu}\left[u\log\left(\frac{\sqrt{1-u^2\cos^2\phi}-u\sin\phi}{\sqrt{1-u^2\cos^2\phi}+u\sin\phi}\right)^2 - \log\left(\frac{\sqrt{1-u^2\cos^2\phi}-\sin\phi}{\sqrt{1-u^2\cos^2\phi}+\sin\phi}\right)^2\right] \tag{36}$$

$$b = a\sec\phi \tag{37}$$

where $u = x/a$ is a dimensionless distance and $\phi = (\pi\sigma/2\sigma_Y)$ is a dimensionless applied load. μ is the shear modulus of the material and $\kappa = (3-\nu)/(1+\nu)$ for plane stress or $\kappa = 3-4\nu$ for plane strain which translates to

$$\frac{(\kappa+1)}{8\pi\mu} = \begin{cases} \frac{1}{\pi E} & \text{plane stress} \\ \frac{1-\nu^2}{\pi E} & \text{plane strain} \end{cases} \tag{38}$$

where E is the modulus and ν is the Poisson's ratio. The key results are:

$$J_p = -\frac{(\kappa+1)\sigma_Y^2 a}{\pi\mu}\ln(\cos\phi) \tag{39}$$

$$A_p = \frac{(\kappa+1)\sigma_Y a^2}{2\pi\mu}\left[2\ln(\cos\phi) + \phi\tan\phi\right] \tag{40}$$

The A_p integral is the more difficult result, but can be solved in *Mathematica* (Wolfram Research, 2001) and has been derived previously (Cherepanov, 1968a; McCartney, 1978). Treating A_p as a function of a and ϕ

$$\frac{dU_{z,ex}}{da} = p\frac{dU_{z,p}}{da} = \frac{p(\kappa+1)\sigma_Y^2 a}{2\pi\mu}\left[4\ln(\cos\phi) + 2\phi\tan\phi + a\frac{d\phi}{da}\left(\phi\sec^2\phi - \tan\phi\right)\right] \tag{41}$$

Substitution into Eq. (11) and solving for $d\phi/da$ leads to the crack propagation law

$$\frac{d\phi}{da} = \frac{\frac{4\pi\gamma\mu}{(\kappa+1)\sigma_Y^2 a} + 2(1+2p)\ln(\cos\phi) + 2p\phi\tan\phi}{ap\left(\tan\phi - \phi\sec^2\phi\right)} \tag{42}$$

It is worth noting that Eq. (42) leads to a Griffith fracture criterion as $\sigma_Y \to \infty$ and reduces to the physically-unreasonable Cherepanov result (Cherepanov, 1968a) when $p = -1$ and $\gamma = \gamma^*$. Also note that while $dU_{z,ex}/da$ and $d\phi/da$ are negative for certain values of a and ϕ, these terms are never negative for values that correspond to physically realizable crack growth. In other words, conditions for crack growth always maintain non-negative $dU_{z,ex}/da$ and $d\phi/da$ as expected for dissipated energy and monotonic crack growth.

First consider the curves that define regions of stable crack growth analogous to those shown schematically in Fig. 2; these curves were calculated by plotting when the numerator in Eq. (42) is zero. Typical plots for a Dugdale material are shown in Fig. 4 for p ranging from 0 to 1. For most crack lengths, this function is double valued. The lower parts of the curves correspond to initiation of fracture and they are nearly independent of p. The upper parts of curves correspond to the onset of unstable crack growth. They decrease to lower stress as p increases. The $p = 0$ curve, which has no plateau, is equivalent to elastic behavior. For $p > 0$ and very short crack lengths, there is a region with no solution. This region corresponds to a material for which the crack can not grow. Physically, it corresponds to a short crack that can not release enough energy to balance the energy dissipated by plastic deformation during crack growth. The material would fail by plastic necking rather than crack growth.

Figure 5 shows the effect of varying the surface energy term γ from 100 J/m^2 down to zero. All these curves were for $p = 1$. The surface energy has little effect on the upper plateau (the onset of unstable crack growth), but has a large effect on the stress for crack initiation. In other words, crack initiation is dominated by having enough energy release to overcome the surface energy term. The $\gamma = 0$ curve is a horizontal line corresponding to the solution to

$$2(1+2p)\ln(\cos\phi) + p\phi\tan\phi = 0 \tag{43}$$

For $p = 1$, the solution is $\phi = 1.18912$ or $\sigma = 0.757\sigma_Y$. In other words, when the surface energy term is small, this analysis predicts unstable crack growth at a constant load that is independent of the initial crack length. Any observed stable crack growth prior to this critical load will be determined by the propagation law in Eq. (42).

Several crack propagation results as a function of the initial crack length are shown superposed on the critical curve with $p = 0.5$ in Fig. 6. These curves were found by numerical solution of Eq. (42). Any curve starting at a_0 rises vertically until it intersects the initiation or lower critical curve. This intersection point was then used as the input boundary condition for solution of the differential equation. Soon after initiation,

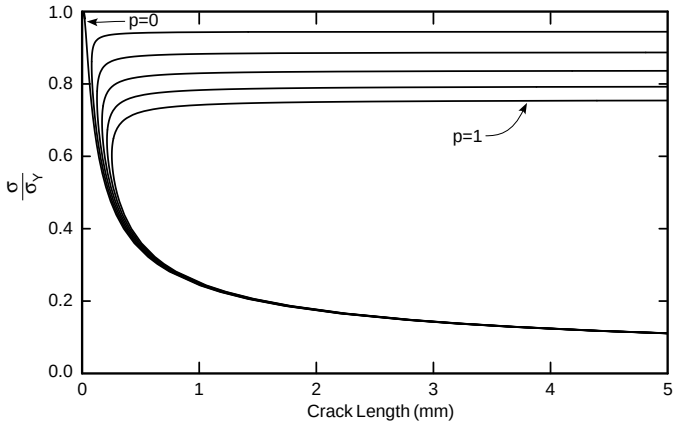

Fig. 4. Critical curves for crack initiation (lower parts of the curves) and unstable crack growth (upper parts of the curves) in a Dugdale material in plane stress with modulus $E = 2500$ MPa and yield stress $\sigma_Y = 50$ MPa. The surface energy was $\gamma = 100$ J/m^2. The different curves are for irreversibility parameters of $p = 0.0$, 0.2, 0.4, 0.6, 0.8, and 1.0.

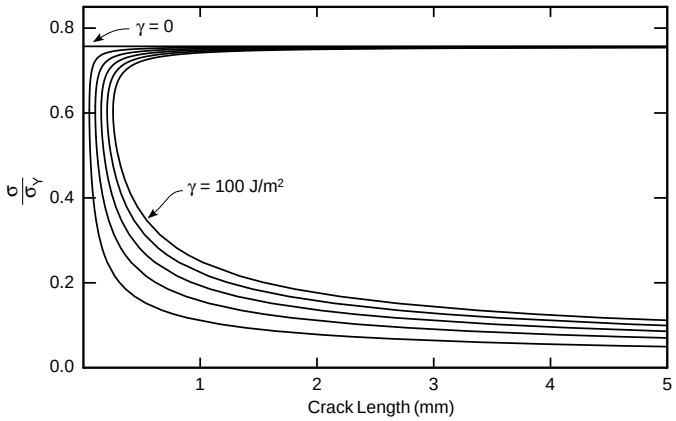

Fig. 5. The effect of surface energy on the critical curves for a Dugdale material in plane stress with modulus $E = 2500$ MPa and yield stress $\sigma_Y = 50$ MPa. The irreversibility parameter was constant at $p = 1$. The different curves are for surface energies of $\gamma = 0$, 20, 40, 60, 80, 100 J/m^2.

all curves have a very short horizontal section because the numerator to Eq. (42) is zero near the critical curves. The propagation curves then all increase rapidly and asymptotically approach the upper critical curve. In this end stage, the crack propagates at constant load, but does not become unstable.

A Virtual Material

A Dugdale material with the crack propagation law in Eq. (42) can be considered a model or virtual material. Given any mode I loading state, because Dugdale yielding is only appropriate for mode I, and a value for the parameter p, one can simulate all aspects of crack initiation and propagation. An interesting application of a virtual material is to build it into structures, such as composites or adhesive joints, and then use simulations to predict the performance of those structures. In this section, the fracture properties of the material itself are considered along with one preliminary result for an adhesive joint. The approach is to conduct fracture experiments by simulation.

In fracture experiments, one loads a specimen until in fails and interprets the fracture properties from the failure results. As shown in the previous section, however, an infinite Dugdale sheet never fails but only reaches a plateau stress accompanied by continued stable crack growth. One approach to characterization of

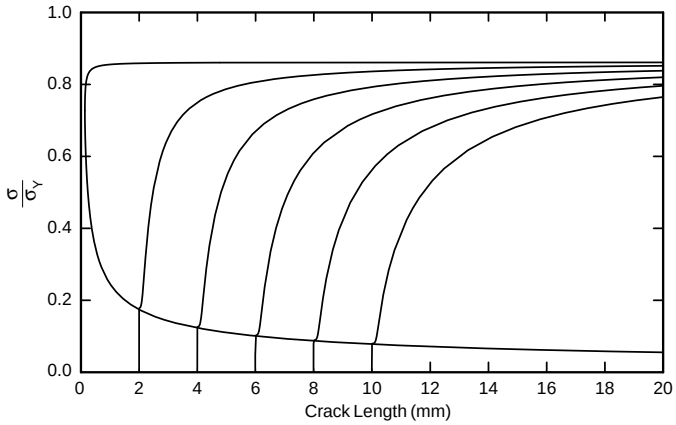

Fig. 6. Crack propagation curves for a Dugdale material in plane stress with modulus $E = 2500$ MPa and yield stress $\sigma_Y = 50$ MPa. The irreversibility parameter was constant at $p = 0.5$. The surface energy was 100 J/m^2. The different curves are for different initial crack lengths of $a_0 = 2$, 4, 6, 8, and 10 mm.

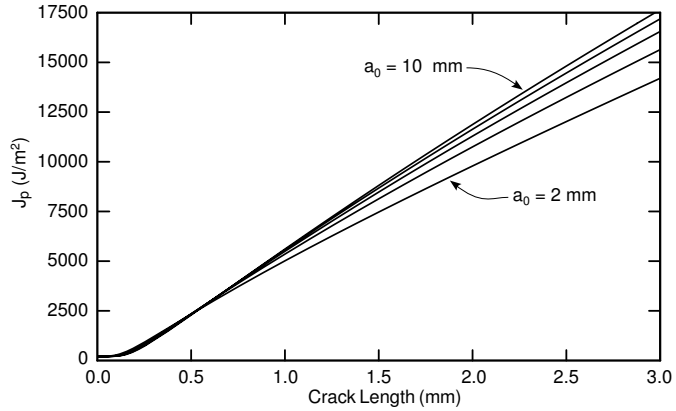

Fig. 7. J_p *vs.* crack growth curves for a Dugdale material in plane stress with modulus $E = 2500$ MPa and yield stress $\sigma_Y = 50$ MPa. The irreversibility parameter was constant at $p = 0.5$. The surface energy was 100 J/m^2. The different curves are for different initial crack lengths.

such materials is to record J_p-Δa curves. Such curves can be calculated from the crack propagation results in Fig. 6 by substituting the stress *vs.* crack length solution into the J_p result (Eq. (39)). The J_p-Δa curves derived from Fig. 6 are shown in Fig. 7. Analogous to real ductile materials, for which the J_p-Δa curve is assumed to be a material property, the J_p-Δa curves in the virtual Dugdale material are independent of initial crack length for the first millimeter of crack growth. At longer crack growths, the curves diverge somewhat with the lower curves being the ones with the shorter initial crack lengths. If the curves were carried out to very large crack growth, the curves would eventually recombine during asymptotic crack growth at constant load. Although the best material characterization for ductile materials may be the full J_p-Δa curve (Rice, 1976), one proposal to get a material constant is the assign the toughness of the material to the J_p value after a fixed amount of crack growth. A proposal in polymer testing has been to treat J_p at 2 mm crack growth as the material toughness (Hale and Ramsteiner, 2001). By this standard, A Dugdale material with $E = 2500$ MPa and $\sigma_Y = 50$ MPa in an infinite sheet under plane stress has a toughness of 8 to 11 kJ/m^2.

The fracture properties change if boundary effects are included by analyzing a finite sheet instead of an infinite sheet. Analysis of a finite sheet requires numerical methods, such as finite element analysis, but as in the infinite sheet analysis, the finite sheet analysis for a Dugdale material can be completed solely with linear-elastic methods; the yield zone can be entered as traction boundary conditions equal to the yield stress. To determine the size of the yield zone, however, an iterative finite element scheme was needed:

1. Select specimen geometry. All calculations here were for rectangular specimens of width $2W$ and length $2L$. The load was applied in the axial direction and the crack of length $2a$ was located in the middle of the specimen. By symmetry, only one quadrant of the sample needed to be analyzed.

2. Select crack length, $2a$, and applied load, σ/σ_Y.

3. The tip of the Dugdale zone must be between $b_{min} = a$ and $b_{max} = W$.

4. Construct finite element mesh for current crack length and yield zone tip $b = (b_{max} + b_{min})/2$. Set applied normal traction equal to σ_Y on the yield zone surface.

5. Run finite element analysis and find both the crack closure work (W_c) (Rybicki and Kanninen, 1977) and the work associated with the tractions on the crack surface (W_T). These energy results are defined by

$$W_c = \lim_{\Delta a\to 0} \frac{1}{2\Delta a}\int_0^{\Delta a} \sigma_{yy}(x-\Delta a)\Delta v(x)dx \quad (44)$$

$$W_T = \lim_{\Delta a\to 0} \frac{1}{2\Delta a}\int_0^{\Delta a} \sigma_Y \Delta v(x)dx \quad (45)$$

   where $x = 0$ is the crack tip, the crack surface is for $x > 0$ and Δa is the size of the crack tip element. A Dugdale solution by finite element analysis is when these two work terms are equal.

6. If $W_c = W_T$ (or sufficiently close), the problem is solved.

7. If $W_c < W_T$, the assumed yield zone was too short. Set $b_{min} = b$ and go back to step 4.

8. if $W_c > W_T$, the assumed yield zone was too long. Set $b_{max} = b$ and go back to step 4.

Step 4 indicates iteration by bisection. As the analysis proceeds and the W_c and W_T results are known for the current b_{min} and b_{max}, efficiency can be improved slightly by converting to a secant of false position method (Press, Flannery, Teukkolsky, and Vetterling, 1988) instead of the bisection method. In these calculations, it typically took 8–10 iterations to converge to the correct yield zone for each selected value of crack length and applied load.

The complete finite element analysis was very tedious. First, crack length was varied for a/W from 0.04 to 0.9. For each crack length the applied load was varied from $\sigma/\sigma_Y = 0.01$ to the plastic collapse load of $1-(a/W)$. A total of 517 crack length/load combinations were run; because each calculation took about 10 iterations, these calculations required over 5000 finite element runs. The entire process was automated using scriptable finite element software (Nairn, 2002). The resulting table of data was numerically differentiated to find the critical points where the numerator in Eq. (42) is equal to zero. The stability envelop for a finite sheet (symbols) are compared to infinite sheet results in Fig. 8. The lower curve for initiation of stable crack growth was unaffected by boundary affects. The upper curve, however, for the onset of unstable crack growth was dramatically affected. In a finite sheet, the upper curve decreased as the crack length approached the width of the specimen. The finite sheet curve is bounded by the plastic limit line for full ligament yielding in the dashed line in Fig. 8. The gap in the finite sheet result at very short crack lengths was a consequence of limitations on extending the FEA mesh to crack tips very close to mesh boundaries. If there were calculations for this region, the symbols would have followed the infinite sheet curve; the justification being that short crack lengths should approach infinite sheet results and that the results before and after the gap are already close to the infinite sheet result.

It is also possible to numerical solve for crack propagation using the table of finite element results. Sample calculations for a finite sheet *vs.* an infinite sheet with an initial crack length of 2mm are shown in Fig. 8. The finite sheet results resemble the infinite sheet results with one major exception. Because of the decreasing upper stability curve, crack growth in finite sheets became unstable when the growth curve intersected that line. This behavior contrasts with infinite sheet results where all crack growth curves asymptotically approached the horizontal critical curve. In infinite sheets, J_p will continue to increase during asymptotic crack growth, but in finite sheets, J_p will have a maximum value defined by the intersection with the upper curve. Figure 9 plots the maximum J_p as a function of final crack length. The maximum J_p for finite sheets

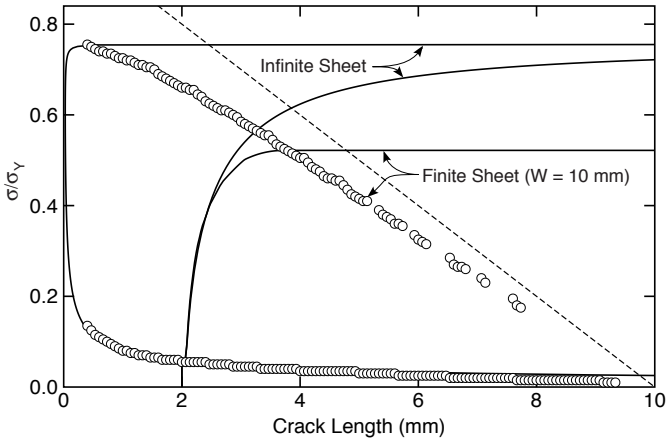

Fig. 8. A comparison of the critical curves for an infinite sheet to those for a finite sheet. The calculations were for a Dugdale material in plane stress with modulus $E = 2500$ MPa and yield stress $\sigma_Y = 50$ MPa. The specimen had $2W = 20$ mm and $2L = 35$ mm. The irreversibility parameter was constant at $p = 1$. The surface energy was 10 J/m^2. The dashed line is the plastic limit for full ligament yielding. The curves starting at $a = 2$ mm are crack growth predictions for infinite and finite sheets.

was close to a material-independent toughness of 4 kJ/m^2 over a wide range of crack lengths (a/W from 0.2 to 0.7). The infinite sheet result is not a critical J_p for unstable crack growth, but rather a plot of $J_p(a, \phi_{crit})$ where ϕ_{crit} corresponds to the asymptotic critical load for an infinite sheet. The infinite sheet result increases with crack length.

The main reason for developing crack simulations in model materials is to do computer experiments on those materials in structures such as crack growth through adhesive joints or in composites and nanocomposites. One preliminary example was to simulate crack growth through a Dugdale material in an adhesive joint. The previous calculations were for a specimen with $2W = 20$ mm and $2L = 30$ mm. This simulation was repeated in specimens where the center of the specimen containing the crack was a Dugdale material of height $2t$ while the remainder of the length ($2(L - t)$) was replaced by steel with $E = 220,000$ MPa and $\nu = 0.2$ (see Fig. 10). For each geometry, the 5000 finite element calculations were run and the results were analyzed to get results for J_p at the onset of unstable crack growth as a function of crack length analogous to the bulk material results in Fig. 9. For all adhesive thicknesses, the central zone was a nearly constant J_p and this critical J_p decreased as the adhesive thickness decreased. The results are summarized in Fig. 10 where they are compared to experimental results on real adhesives from Bascom, Cottington, Jones, and Peyser (1975). There was no expectation that a Dugdale material will reproduce real experiments; all that was considered was whether or not simulations in model materials can reproduce scaling effects in real adhesives. To check for modeling of scaling effects, and to make it possible to make comparisons, both the simulation results and the experimental results were normalized. The toughnesses were normalized to the toughness of the bulk material; the thicknesses were normalized to the observed thickness required to cause 50% reduction in toughness. In the normalized comparison, the simulation results agree well with experimental trends.

The Dugdale model can be characterized as a cohesive zone model with a rigid-plastic, crack-tip force-displacement law (Williams, 2002). Despite this characterization, the fracture simulations in this section that use a Dugdale model have nothing in common with numerical crack growth models based on cohesive zones. A cohesive zone model with Dugdale yield zones would predict crack propagation when the area under the crack-tip, force-displacement law equals an input toughness property. Use of such a model for the problems in this section would find J_p during crack growth to be equal to the input toughness for all crack lengths and for all adhesive thicknesses. In the new class of fracture methods proposed here — fracture simulations — the crack grows by energy balance conditions and the simulation results are examined to find the value of J_p that was present during that crack growth. Because J_p is a simulation result and not an input parameter, it is possible to study effects such as the effect of adhesive thickness on the fracture toughness of the material.

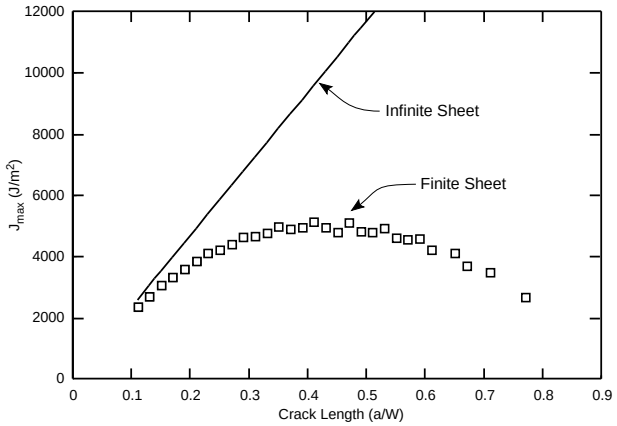

Fig. 9. The total J_p at the onset of unstable crack growth in a finite sheet compared to the corresponding J_p in an infinite sheet at the same crack length.The calculations were for a Dugdale material in plane stress with modulus $E = 2500$ MPa and yield stress $\sigma_Y = 50$ MPa. The irreversibility parameter was constant at $p = 1$. The surface energy was 10 J/m^2.

Conclusions

An examination of the thermodynamics of crack growth in elastic-plastic materials showed that it is possible to develop a virtual material that exhibits crack growth by balance of energy released with energy required for crack growth. It was insufficient to balance energy using traditional plastic-flow methods. Instead, the energy balance needed to include some model for extra irreversible energy effects. The calculations of this paper provide just one example of developing a virtual material based on a specific plasticity model — a Dugdale material — and using one model for irreversible energy — proportional to plastic-flow energy in an elastic-plastic stress analysis. There is no claim that a Dugdale material is a realistic virtual material that should be used for modeling ductile fracture or that physical basis has been demonstrated for the irreversible energy term. The calculations do, however, demonstrate that energy-balance crack simulations are possible. Furthermore, it is encouraging that this first attempt has many properties similar to real ductile crack growth. It has a load to initiate crack growth, followed by a period of stable crack growth. There is a stability criterion which may or may not lead to unstable crack growth depending on material properties and geometry. Some ductile fracture parameters are nearly material constants. For example, the $J_p - \Delta a$ curve is a material property for the first stages of crack growth and the critical J_p for unstable crack growth is a material constant for finite sheets over a wide range of initial crack lengths. Finally. the toughness of a virtual Dugdale material in an adhesive joint decreases with joint thickness by a similar trend to real adhesives.

There are, however, several deficiencies. For example, the toughness increases as the yield stress of the material increases. All results scale with σ/σ_Y. In other words, as the yield stress of the material increases, the analysis results remain unchanged. The only affect of increasing σ_Y is that the final values for J_p will increase. In real materials, increasing σ_Y will eventually cause a transition from ductile behavior to brittle behavior. A Dugdale material can not capture this effect. Two possible reasons are that the Dugdale model is an oversimplification of the yielding process or that the irreversibility parameter, p, is a function of σ_Y. Perhaps improved plasticity models will increase the realism of the simulations. Note that the proposed model for irreversible energy dissipation is general and thus the approach of this paper can be adapted to more realistic plasticity models and to new models for irreversible energy effects. The Dugdale model was used here only because it allows analytical solutions for some results. A transition to brittle behavior can be simulated, even in a Dugdale material, by having p decrease toward zero as σ_Y increases. This approach would require more assumptions about the material or perhaps some experimental results to have results for p. The benefits of pursuing more realistic virtual materials is that they could be used in computer experiments to provide more realistic analysis of complex crack growth problems. Extension to

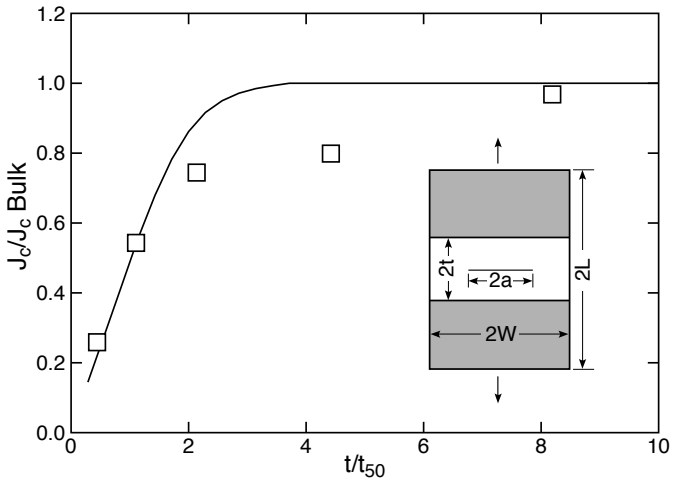

Fig. 10. The critical J_p as a function of adhesive thickness for a Dugdale material between steel adherends (line) compared to experimental results (symbols) from Bascom, Cottington, Jones, and Peyser (1975). For comparison, the simulation J_c was normalized to the bulk $J_c = 5200$ J/m^2 and simulation thickness was normalized to the thickness causing 50% toughness loss ($t_{50} = 3.5$ mm). Similarly, the experimental results (symbols) were normalized to bulk $J_c = 2600$ J/m^2 and $t_{50} = 0.118$ mm. The inset figure shows the specimen geometry for the FEA calculations.

more advanced plasticity models will also require more efficient numerical methods that can include energy dissipation materials. Work on the numerical methods for fracture simulations is in progress.

Acknowledgements

The work was supported by a grant from the Department of Energy DE-FG03-02ER45914 and by the University of Utah Center for the Simulation of Accidental Fires and Explosions (C-SAFE), funded by the Department of Energy, Lawrence Livermore National Laboratory, under Subcontract B341493.

References

Atkins, A. G., 1999. Scaling Laws for Elastoplastic Fracture, *Int. J. of Fract. 95*, 51.

Barenblatt, G. I., 1962. The Mathematical Theory of Equilibrium Cracks in Brittle Fracture, *Adv. Appl. Mech. 7*, 55.

Bascom, W. D., R. L. Cottington, R. L. Jones, and P. Peyser, 1975. The Fracture of Epoxy- and Elastomer-Modified Epoxy Polymers in Bulk and as Adhesives, *J. Appl. Polym. Sci. 19*, 2545.

Becker, Wilfred, 1997. Closed-Form Modeling of the Unloaded Mode I Dugdale Crack, *Eng. Fract. Mech. 57*, 355.

Cherepanov, G. P., 1968a. On Quasibrittle Fracture, *Prikladraya Mat. Mechanika 32*, 1034.

Cherepanov, G. P., 1968b. Cracks in Solids, *Int. J. Solids & Struct. 4*, 811.

Dugdale, D. S., 1960. Yielding of Steel Sheets Containing Slits, *J. Mech. Phys. Solids 8*, 100.

Gaskell, D. R., 1995. *Introduction to the Thermodynamics of Materials*, Taylor & Francis, Washington, DC.

Hale, G. E. and F. Ramsteiner, 2001. J-Fracture Toughness of Polymers at Slow Speeds, *Fracture Mechanics Testing Methods for Polymers Adhesives and Composites*, eds., D. R. Moore, A. Pavan, J. G. Williams, ESIS Publication 28, Elsevier, 123.

Hill, R., 1983. *The Mathematical Theory of Plasticity*, Oxford, Clarendon Press, New York.

Hunston, D. L., 1984. Composite Interlaminar Fracture: Effect of Matrix Fracture Energy, *Comp. Tech. Rev. 6*, 176.

McCartney, L. N., 1978. Theory of Stable Crack Growth in an Elastic-Perfectly Plastic Material, *Int. J. Fract. 14*, 429.

Mostovoy, S. and E. J. Ripling, 1966. Fracture Toughness of an Epoxy System, *J. Appl. Polym. Sci. 10*, 1351.

Mostovoy, S. and E. J. Ripling, 1971. Effect of Joint Geometry on the Toughness of Epoxy Adhesives, *J. Appl. Polymer Sci. 15*, 661.

Nairn, J. A., 2000. Matrix Microcracking in Composites, *Polymer Matrix Composites*, eds., R. Talreja and J.-Å. E. Manson, Vol. 2 of Comprehensive Composite Materials, Elsevier Science, 403.

Nairn, J. A., 2002. JANFEA: Finite Element and Material Point Method Software for the Macintosh, `http://www.mse.utah.edu/~nairn/JANFEA`.

Press, W. H., B. P. Flannery, S. A. Teukolsky, and W. T. Vetterling, 1988. *Numerical Recipes in C: The Art of Scientific Computing*, Cambridge University Press, New York.

Rice, J. R., 1968. A Path Independent Integral and the Approximate Analysis of Strain Concentration by Notches and Cracks, *J. Applied Mech. June*, 379.

Rice, J. R., 1976. Elastic-Plastic Fracture Mechanics. *ASME Winter Annual Meeting*, Ed., F. Erdogan, New York, NY, Dec 5-10, 1976.

Ripling, E. J., S. Mostovoy, and R. L. Patrick, 1964. Measuring Fracture Toughness of Adhesive Joints, *Materials Research & Standards 4*, 129.

Rybicki, E. F. and M. F. Kanninen, 1977. A Finite Element Calculation of Stress Intensity Factors By a Modified Crack Closure Integral, *Eng. Fract. Mech. 9*, 931.

Tvergaard, V. and J. W. Hutchinson, 1992. The Relation Between Crack Growth Resistance and Fracture Process Parameters in Elastic-Plastic Solids, *J. Mech. Phys. Solids 40*, 1377.

Williams, J. G., 1984. *Fracture Mechanics of Polymers*, John Wiley & Sons, New York.

Williams, J. G., 2002. Analytical Solutions for Cohesive Zone Models, *J. Mech. Phys. Solids 50*, 809.

Wolfram Research, Inc., 2001. Mathematica 4.0, Champaign, IL.

Wnuk, M. P., 1971. Subcritical Growth of Fracture, *Int. J. Fract. Mech.* 7, 383.